Journal of Alloys and Compounds 504 (2010) 197–200

Contents lists available at ScienceDirect

Journal of Alloys and Compounds

journal homepage: www.elsevier.com/locate/jallcom

Optical features of $Ca_4NdO(BO_3)_3$:Yb single crystals under CW laser illumination

A. Wojciechowski[a], M. Swirkowicz[b], A. Karas[b], L.R. Jaroszewicz[c], A. Majchrowski[c], E. Gondek[d], K. Ozga[e], I.V. Kityk[a,*]

[a] *Electrical Engineering Department, Czestochowa Technological University, Armii Krajowej Av. 17/19, Czestochowa, Poland*
[b] *Institute of Electronic Materials Technology, Wolczynska 133, 01-919 Warsaw, Poland*
[c] *Institute of Applied Physics, Military University of Technology, Gen. Sylwestra Kaliskiego 2, 00-908 Warsaw, Poland*
[d] *Institute of Physics, Cracow University of Technology, Podchorążych St. 1, Cracow 30-084, Poland*
[e] *Public Health, Czestochowa Technological University, Armii Krajowej Av. 36B, 42-200 Czestochowa, Poland*

ARTICLE INFO

Article history:
Received 18 March 2010
Received in revised form 10 May 2010
Accepted 14 May 2010
Available online 27 May 2010

Keywords:
Borate crystals
Optical materials

ABSTRACT

Optical treatment of $Ca_4NdO(BO_3)_3$:Yb under continuous laser illumination at different wavelengths led to substantial changes of optical absorption and optical second harmonic generation. The treatment was performed successively by infrared (780 nm), red (650 nm), green (532 nm) and blue (405 nm) laser wavelengths with powers varying within the 200–400 mW range. We demonstrated enhancement of the optical second harmonic generation in the $Ca_4NdO(BO_3)_3$:Yb (1.9% in weighting unit) crystals under the influence of the green cw laser at 532 nm. The principal changes were observed after 15 min of the treatment. A correlation between the occurrence of the hyperfine structure in the absorption spectra and the enhancement of the optical second harmonic generation was found. The additional treatment by the blue laser led to disappearance of appeared photo-induced changes of absorption and decrease of the optical second harmonic generation. It is principal that the effect is non-reversible in time and it does not depend on the photo-inducing light polarization.

The principal origin of the observed photo-induced optical second harmonic generation is photo-polarization of the particular rare earth localized levels and formation of the stable polarized states due to the presence of Yb ions, playing crucial role. No such effects were observed in pure $Ca_4NdO(BO_3)_3$.

1. Introduction

Recently there is observed a great interest in producing materials which are laser operable [1,2]. The principal mechanisms are based on formation of the photo-induced non-centrosymmetry and formation of the photo-induced gratings [3]. Particular interest present here rare earth doped borates [4,5]. Most of the present studies were done during the treatment by the pulsed lasers [6], which required stabilization of the power densities using for the treatment. In order to search novel promising materials it is necessary to have high quality optical crystals where the photo-induced changes may be reproducible with high accuracy. Due to exceptional stability and possibility of introducing different rare ions the oxoborates, with the composition Ca_4 $REO(BO_3)_3$ where RE = Gd, Y, Nd are very promising materials [7,8]. The coexistence of the Nd and Yb rare earth ions in borate matrices is of particular interest [9]. In our recent work [10] we have shown that even illumination by single-pulsed Nd:YAG laser pulses during the usual second harmonic process causes a substantial changes of fundamental inter-band absorption. It is principal that in the Yb ions there are not any signs of excitation absorption and multi-photon processes. In this work we study influence of successive cw laser treatment by different wavelengths beginning from infrared through red, green up to blue (405 nm) on the absorption and second order susceptibilities such as optical second harmonic generation (SHG). The presence of two rare earth ions in the crystal lattice may be a principal factor for realization of effective energy transfer processes [11,12]. Therefore we will study the changes of linear and nonlinear optical susceptibilities under influence of the cw laser illumination. The effects should be very sensitive to the laser wavelengths and time of illumination. The photo-induced changes may be preliminary caused by the long-living metastable states formed by the localized rare earth energy levels effectively interacting with the phonon subsystem. We will study the changes of the mentioned optical features after the cw treatment and we will explore the role of particular intra-band transitions responsible for the effect.

---

[*] Corresponding author.
E-mail addresses: ikityk@el.pcz.czest.pl, iwank74@gmail.com (I.V. Kityk).

0925-8388/$ – see front matter © 2010 Elsevier B.V. All rights reserved.
doi:10.1016/j.jallcom.2010.05.087

2. Technology of single crystal growth and method of its characterization

$Ca_4NdO(BO_3)_3$ (NdCOB), like other rare earth calcium oxoborates (GdCOB, YCOB) melts congruently at 1470 °C. Between the crystallization and room-temperature there are no irreversible or destructive phase transitions, so the material can be grown by means of standard Czochralski technique. Neodymium sites can be substituted with other rare earth ions such as Yb^{3+} and in this way the ytterbium doped NdCOB single crystals were obtained. The growth was carried out from an iridium crucible (50 mm × 50 mm in height and diameter) covered with active iridium after heater and alumina tubes to diminish the steep temperature gradients in the furnace caused by inductive heating. The Oxypuller 05-03 equipment made by Cyberstar and inductive Hüttinger generator were used. The nitrogen atmosphere containing 1 vol.% of oxygen was used to prevent etching of the surfaces of the growing crystals. As-grown single crystals were up to 50 mm in length and had rhombus cross-section 21 mm × 24 mm. The detailed description of the used technology can be found elsewhere [10]. The microstructural analysis has shown that the investigated samples had 1.9% of Yb^{3+} in the weighting units.

For the photo-inducing treatment we have used cw lasers with powers varying within the range from 200 mW up to 400 mW. The laser beam has diameters equal to about 2 mm and the following wavelengths: infrared (780 nm), red (660 nm), green (532 nm), blue 405 (nm). The optical SHG was measured for the pulsed 10 ns Erbium glass laser with power densities up to $1.2\,GW/cm^2$. The fast response photo-detector together with interferometric filter at 770 nm were applied for detection of the output SHG. The photo-inducing laser beam has incident on the surface of the samples under the angles within the 20–30°. The SHG was measured during the rotation ion the crystallographic *XZ* planes.

For control of the surfaces we have done measurements of the optical constants using ellisometrical methods. Spectroscopic ellipsometry measures (ψ, Δ) spectra for photon energy or wavelength. In general, the interpretation of measurement results is rather difficult from the absolute values of (ψ, Δ). From this data analysis, physical properties including the optical constants and film thicknesses of the sample can be extracted. Unlike reflectance measurement, ellipsometry allows the direct measurement of the refractive index n and extinction coefficient k. The M-2000^{TM} D2 and QTH Light Source houses the Deuterium and Quartz Tungsten Halogen lamps. The power for the lamp is supplied through highly switching DC power supplies that are located in the M-2000^{TM} XLS light source. 24 V is provided to it from the Detector and Lamp Power Supply Module. This unit also contains the beam collimation optics, a fixed polarized, and a compensator located in a continuously rotating stepper motor. The deuterium Lamp Supplies light from the UV to the visible region was applied. The lamp is mounted just behind the shutter aperture. The Quartz Tungsten Halogen Lamp supplied light from the visible to the IR region of the spectrum.

The measurements were done using Variable Angle Spectroscopic Elipsometry—VASE (J.A. Woollam) set-up for different incident angles. The samples were measured within the spectral range 180–1700 nm at three different angles. The fitting procedure was performed by Complete Ease program with using of Cauchy model, which describes the refractive index dispersion by an equation:

$$n(\lambda) = A_n + \frac{B_n}{\lambda^2} + \frac{C_n}{\lambda^4} + \frac{D_n}{\lambda^6} \ldots$$

where A_n, B_n, C_n are the fitting parameters for the wavelength λ.

The values of n and k were evaluated by method of mathematical regression within a framework of Mean Squared Error (MSE). Additionally it was evaluated the surface roughness. The obtained by this method dispersion for the refractive indices and absorption coefficients are given in Fig. 1. The evaluated fitting parameters of the Couchy models corresponded to $A = 1.701 \pm 0.00065791$; $B = 0.00834 \pm 0.00041334$; $C = -0.00021638 \pm 4.9460E\text{-}05$; $D = 1.2963E\text{-}05 \pm 1.4782E\text{-}06$ spectrum.

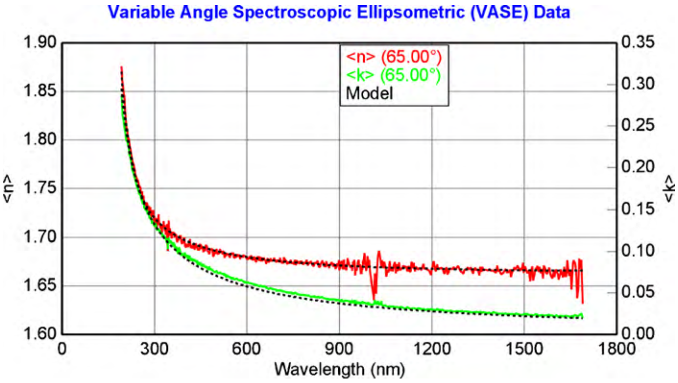

Fig. 1. Principal dispersion of refractive indices and absorption coefficients.

We have established that the effective refractive indices are very stable and are almost independent on the Yb^{3+} content. The surface roughness indicates on a high quality of the sample surface playing crucial role during the illumination.

3. Results and discussion

Fig. 2 presents the typical non-polarized room-temperature absorption spectra of the studied crystals obtained at spectral resolution about 1 nm together with the principal spectral bands identifications. One can see that the half-widths of the spectral lines are sufficiently small, what indicates on a relatively stable local sites of the particular rare earths ions [13]. Their identification clearly shows that the dominant contribution originates from Nd ions. Changes of the Yb^{3+} ion content did not play substantial role in the spectral positions of the absorption peaks, however there are some changes in the relative intensities.

In Fig. 3 the photo-induced changes of the absorption obtained during the successive treatment of the sample's surfaces are presented. The illumination has been started from infrared laser wavelength ($\lambda = 785$ nm), after it was continued using successive

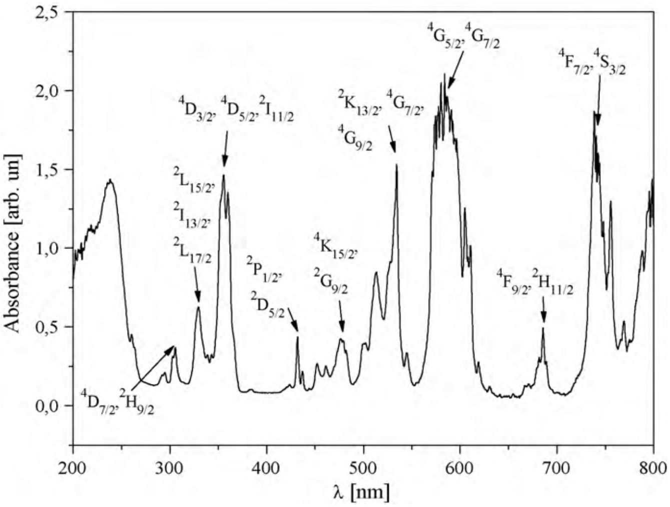

Fig. 2. Unpolarized UV–vis absorption spectrum of $Ca_4NdO(BO_3)_3$:Yb.

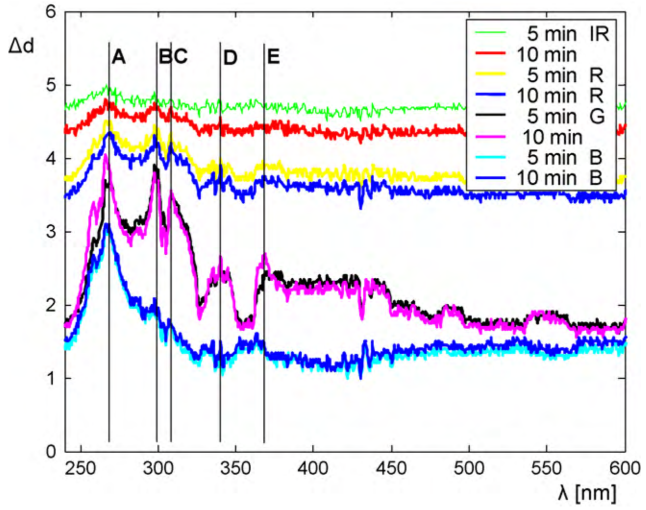

Fig. 3. Photo-induced absorption during successive treatment IR → red → green → blue.

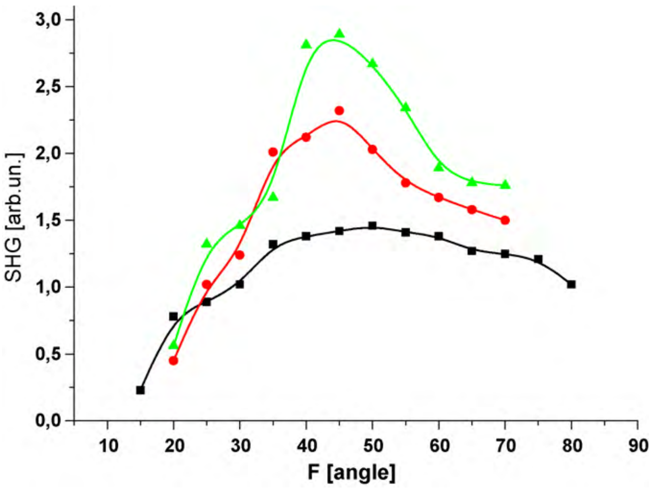

Fig. 4. Angle dependence of the SHG at the laser line 1320 nm: triangles correspond to the optical treatment by cw green laser line; diamonds to infrared 790 nm and red 660 nm laser treatment; squares to blue laser treatment.

illumination by red laser line ($\lambda = 660$ nm), green line ($\lambda = 532$ nm), and finally by blue line ($\lambda = 405$ nm). The illuminated power was equal to about 200 mW and beam spot diameter was equal to about 1.5 mm. The changes of the optical absorption (cw laser induced absorption) are more pronounced during the green laser ($\lambda = 532$ nm) treatment. One can see occurrence of at least five sharp spectral peaks marked as *A*, *B*, *C*, *D*. Moreover the changes under illumination by green laser line treated surfaces seem to be sufficiently stronger with respect to the IR laser treatment. In the observed photo-induced absorption one can see substantial contribution originating caused by $4I_{9/2}$ to $4K_{15/2}$, $2G_{18/2}$, $2K_{13/2}$, $4G_{7/2}$, $4G_{11/2}$, $4I_{9/2}$, $4G_{5/2}$, $4G_{7/2}$ transitions. Besides the optical treatment [14], giving variations of the absorption immediately after the treatment it would be very interesting to explore the behavior of the photoabsorption after the switching off the cw laser treatment.

It is necessary to emphasize that the cw laser powers were far from melting point's temperatures, however they were sufficiently strong to produce the observed effects. The mentioned photo-induced absorption may be caused by resonance excitations of the Nd localized states. The successive enhancement of the laser's treatment time causes substantial redistribution of the localized electron occupation. More sensitive to the laser treatment are transitions from $4I_{9/2}$ to $4D_{3/2}$, $4D_{5/2}$, $4I_{11/2}$, and $4D_{1/2}$ states. The process shows a behavior similar to usual photo-polarization. At the same time the monitoring of the illuminated surfaces do not show any signs of photo-stimulated crystallization. Following the Ref. [15] it may be appeared only during photo-treatment by focused 0.7 W cw laser beam with μm diameter spots. The observed process is different from the pulse laser treatment because in our case we have substantially equilibrium processes during the photo-treatment below the crystallization processes and absence of the non-equilibrium structural components. It is also crucial that the considerable changes are observed after 15 min of the illumination. And the local heating do not exceed 3.4 K following the laser pirometer control. So one can assume a formation of the long-living photo-induced trapping metastable levels, which due to additional broadening caused by slow thermoheating play significant role in the observed effects [16]. As a confirmation the further treatment by the red laser demonstrates the behavior similar the infrared laser line.

One can expect that irradiation by the laser lines outside the absorption spectral bands (Fig. 1) effectively depopulate some photo-occupied metastable localized states as it was observed for the case of photo-induced Frenkel defect states [17]. The appeared photo-induced absorption bands are only slightly time relaxed: relaxation of the stimulated absorption does not exceed 15% after several days.

The behavior of the angle-dependent SHG during 1064 nm, 10 ns pulse treatment in the *XZ* crystallographic plane is presented in Fig. 4. One can see that maximal increase of the SHG output appear after 15 min of the green laser treatment. The effect is maximal for the s-p SHG configurations and generally is similar to the one observed previously [18].

The 405 nm laser leads to substantial decrease of the output SHG, what correlates with the behavior of the photo-induced absorption. At the same time some shift of the angle corresponding to maximum SHG is observed together with the modifications of the SHG shape.

4. Conclusions

We demonstrated enhancement of the optical second harmonic generation in the $Ca_4NdO(BO_3)_3$:Yb (1.9% in weighting unit) crystals under the influence of the green cw laser at 532 nm. A correlation between the occurrence of the hyperfine structure in the absorption spectra and the enhancement of the optical second harmonic generation was found. The additional treatment by the blue laser led to disappearance of appeared photo-induced changes of absorption and decrease of the optical second harmonic generation. It is principal that the effect is non-reversible in time and it does not depend on the photo-inducing light polarization.

The principal changes were observed after 15 min of the treatment. The changes are maximal during treatment by green 532 nm laser beam and are substantially less during 780 nm laser treatment. One can see substantial contribution to photo-induced absorption due to transition from $4I_{9/2}$ to $4D_{3/2}$, $4D_{5/2}$, $4I_{11/2}$, and $4D_{1/2}$ states. The mentioned photo-induced absorption may be caused by resonance excitations of the Nd localized states. The successive enhancement of the laser power causes sufficiently clear redistribution of the starting electron occupation where the principal role play transitions from $4I_{9/2}$ to $4D_{3/2}$, $4D_{5/2}$, $4I_{11/2}$, and $4D_{1/2}$ electronic states.

Acknowledgements

The authors appreciate the financial support of the Polish Ministry of Sciences and Higher Education, Key Project POIG.01.03.01-14-016/08 “New Photonic Materials and their Advanced Applications”.

References

[1] T. Oikawa, T. Honma, T. Komatsu, Cryst. Res. Technol. 43 (2008) 1253.
[2] A. Majchrowski, M. Swirkowicz, K. Ozga, I.V. Kityk, Opt. Commun. 283 (2010) 1378.
[3] R. Miedzinski, J. Ebothé, G. Kozlowski, J. Kasperczyk, I.V. Kityk, I. Fuks-Janczarek, K. Nouneh, M. Oyama, M. Matusiewicz, A.H. Reshak, Superlattice Microstruct. 46 (2009) 637.
[4] L.I. Isaenko, A.P. Yelliseev, Chem. Sust. Dev. 8 (2000) 217.
[5] J. Ebothe, I.V. Kityk, J. Kisilewski, T. Lukasiewicz, R. Diduszko, A. Majchrowski, Appl. Phys. Lett. 89 (2006) 131106.
[6] H. Nakao, Y. Ruan, H. Furuya, I. Yamada, M. Yoshimura, Y. Mori, T. Sasaki, Jpn. J. Appl. Phys. 39 (2000) L463.
[7] G. Aka, E. Reino, P. Loiseau, D. Vivien, B. Ferrand, L. Fulbert, D. Pelenc, G. Lucas-Leclin, P. Georges, Opt. Mater. 26 (2004) 431.
[8] H. Takeda, H. Nakao, S. Izukawa, H. Shimiru, T. Nishida, S. Okamura, T. Shiosaki, J. Alloys Compd. 408–412 (2006) 474.
[9] M.O. Ramirez, D. Jaque, L.E. Bausa, I.R. Martin, F. Lahoz, E. Cavali, A. Speghini, M. Betinelli, J. Appl. Phys. 97 (2005) 093510.
[10] A.H. Reshak, A. Majchrowski, M. Swirkowicz, A. Klos, T. Lukasiewicz, I.V. Kityk, K. Iliopoulos, S. Couris, M.G. Brik, J. Alloys Compd. 481 (2009) 14.
[11] A. Kaminskii, Crystalline Lasers: Physica Processes and Operating Schemes, CRC, Boca Raton, FL, 1996;
C. Honninger, F. Morier-Genoud, M. Moser, U. Seller, L.R. Brovelli, C. Harder, Opt. Lett. 23 (1998) 126.
[12] A. Majchrowski, L.R. Jaroszewicz, M. Swirkowicz, R. Miedzinski, M. Piasecki, I.V. Kityk, A. Wojciechowski, M.G. Brik, Mater. Lett. 64 (2009) 295.
[13] L. Xiuai, Y. Zhenyu, L. Jianfu, Z. Zhaojie, J. Guohua, W. Yan, W. Baichang, T. Chaoyang, J. Cryst. Growth 281 (2005) 416.
[14] J. Sablayrolles, V. Jubera, M. Delaigue, I. Manek-Hönninger, J.-P. Chaminade, J. Hejtmanek, R. Decourt, A. Garcia, Mater. Chem. Phys. 115 (2009) 512.
[15] T. Honma, Y. Benino, T. Fujiwara, R. Sato, T. Komatsu, Nippon Reramikkusu Kyokai Aakujutsu Ronbunshi 110 (2002) 398 (in Japanese).
[16] M.A.K. Elfayoumi, M. Farouk, M.G. Brik, M.M. Elokr, J. Alloys Compd. 492 (2010) 712.
[17] M. Idrish Miah, Phys. Lett. 374 (2009) 75.
[18] K. Hussain, P. Kumbhakar, Braz. J. Phys. 36 (2006) 12.